

Stripe order enhanced superconductivity in the Hubbard model

Hong-Chen Jiang^{a,1} and Steven A. Kivelson^{b,1}

^aStanford Institute for Materials and Energy Sciences, SLAC National Accelerator Laboratory and Stanford University, Menlo Park, California 94025, USA; ^bDepartment of Physics, Stanford University, Stanford, California 94305, USA

This manuscript was compiled on January 5, 2022

Unidirectional (“stripe”) charge-density-wave order has now been established as a ubiquitous feature in the phase diagram of the cuprate high temperature (HT) superconductors, where it generally competes with superconductivity (SC). None-the-less, on theoretical grounds it has been conjectured that stripe order (or other forms of “optimal” inhomogeneities) may play an essential positive role in the mechanism of HTSC. Here we report density matrix renormalization group studies of the Hubbard model on long 4 and 6 leg cylinders where the hopping matrix elements transverse to the long direction are periodically modulated - mimicing the effect of putative period-2 stripe order. We find even modest amplitude modulations can enhance the long-distance SC correlations by many orders of magnitude, and drive the system into a phase with a substantial spin gap and SC quasi-long-range-order with a Luttinger exponent, $K_{sc} \sim 1$.

Hubbard model | Superconductivity | stripe order

A complex relation between multiple ordering tendencies appears to be a universal feature of highly correlated electronic systems(1). For example, charge-density-wave (CDW), spin-density-wave (SDW), and d-wave superconducting (SC) orders all arise in significantly overlapping regimes of the phase diagram of the cuprate high temperature superconductors. Moreover, studies of the Hubbard model with repulsive U of order the band-width, $U \sim W$, have been difficult to interpret unambiguously, in large part because these same ordering tendencies appear to be in delicate balance with one another(2, 3).

There are clear senses in which these orders “compete”: This can be seen phenomenologically in the cuprates where suppressing SC order with a magnetic field enhances the strength of the observed CDW, and where the most robust SC often appears in regions of the phase diagram where the CDW order is relatively weaker(4). A similar feature is vividly apparent in density matrix renormalization group (DMRG) studies of the the Hubbard model on long but relatively narrow cylinders and ladders(5–17). Here, the closest possible approximation of a SC state is a Luther-Emery liquid,(18) in which the SC and CDW susceptibilities are determined by quantum mechanically dual variables. Thus, any change in the parameters - e.g. details of the band-structure or the strength of the interactions - that enhances the long distance correlations of one necessarily decreases the other. It has even been suggested that this competition is so ferocious that the Hubbard model with $U \sim W$ may never be superconducting in the 2d limit.(14)

However, the fact that high temperature superconductivity and CDW (not to mention SDW) orders all seem to appear together suggests that they may be linked in a more multifaceted manner than the word “competing” suggests.(19) Indeed, two distinct theoretical proposals carry the implication that CDW order can enhance SC: 1) It was proposed in Ref.

(20, 21) that CDW fluctuations - associated with proximity to a putative CDW quantum critical point - could serve as an effective pairing “glue” and thereby enhance SC even under conditions in which fully developed CDW order might depress SC by opening gaps on portions of the Fermi surface. 2) It was proposed in Ref. (22), and further developed in a variety of subsequent papers(23–28), that static or slowly fluctuating CDW order could produce a form of “optimally inhomogeneous” electronic structure that could enhance SC.

In the present paper, we use DMRG studies of the square lattice Hubbard model on 4 and 6 leg cylinders with length $L_x = 32$ and 48 to explore the second of these propositions. We consider the model with only nearest-neighbor interactions t , with $U = 12t$, and for electron density per site $n = 1 - \delta$ with $\delta = 1/8$ and $1/12$. Moreover, we assume an ordered period 2 explicit CDW with ordering vector perpendicular to the long axis of the cylinder, so that the hopping-matrix elements in this direction are alternately enhanced or depressed, $t \rightarrow t \pm dt$ as shown in Fig.1.

For $dt = 0$ this is the uniform Hubbard model, which in this range of parameters appears(9–11, 14, 15) to favor an insulating phase with spontaneous translation symmetry breaking corresponding to an array of “full stripes,” i.e. the CDW period along the cylinder is $\lambda_{cdw} = 1/\delta$.(29–31) As might be expected, this state has exponentially falling SC correlations at long distances. For $dt = t$, this system consists of decoupled

Significance Statement

The Hubbard model plays a central role in the theory of highly correlated systems. Its simplicity allows conceptual issues – which are generally complicated in the context of experiments on interesting materials – to be sharply posed and definitively answered. Recently, a variety of numerical studies have led to the conclusion that the “pure” Hubbard model on the square lattice at intermediate coupling, U , is not superconducting in the range of electron densities in which many previous approximate treatments had inferred high temperature superconductivity. Here, using controlled density-matrix renormalization group methods, we show that superconductivity is spectacularly enhanced if the hopping matrix elements are periodically modulated in a stripe-like pattern, with important (if suggestive) implications concerning the mechanism of unconventional superconductivity.

Author contributions: H.C.J. and S.A.K. designed research; H.C.J. performed the DMRG simulation and analyzed data; and H.C.J. and S.A.K. wrote the paper.

The authors declare no conflict of interest.

¹To whom correspondence should be addressed. E-mail: hcjiang@stanford.edu or kivelson@stanford.edu.

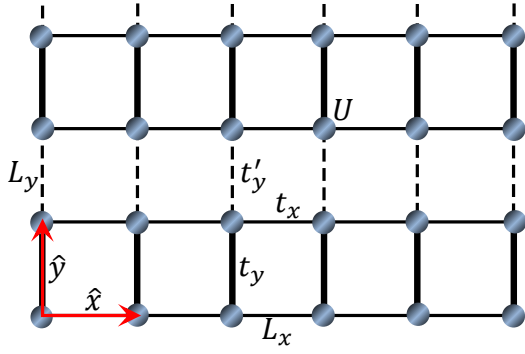


Fig. 1. Hubbard model on the square cylinder. Periodic and open boundary conditions are imposed, respectively, along the directions specified by the lattice basis vectors $\hat{y} = (0, 1)$ and $\hat{x} = (1, 0)$. $t_x = t$ and $t_y = t + dt$ ($t'_y = t - dt$) are hopping integrals between nearest-neighbor sites in the \hat{x} and \hat{y} directions. U is the on-site Coulomb repulsion, L_x and L_y are the number of sites.

2-leg ladders. While the behavior of the 2-leg ladder depends on the ratio of t_y/t_x , so long as this ratio does not exceed a critical value(16), the 2-leg ladder is known(16, 23, 32–34) to support a Luther-Emery liquid phase with power law SC correlations that fall with distance r as $|r|^{-K_{sc}}$ with K_{sc} between 1 and 2.* Here, we explore the effect of relatively weak modulations, $dt \leq 0.4$.

In all cases we find that the modulation enhances the SC correlations at long distances relative to the uniform cylinder ($dt = 0$) by many orders of magnitude. Indeed, the modulated cylinder seemingly forms a Luther-Emery liquid: The spin-spin correlator and the single-particle Green function fall exponentially with distance with a correlation length of order a lattice constant, indicating the existence of a spin gap. Moreover, there are clear CDW correlations with wavelength $\lambda_{cdw} = 1/2\delta$ for the 4 leg and $\lambda_{cdw} = 2/3\delta$ for the 6 leg cylinder. However, while it is plausible that they also have power-law correlations characterized by Luttinger exponent K_{cdw} , the expected duality relation $K_{cdw} = 1/K_{sc}$ is only barely consistent with the DMRG results for the 4-leg and clearly inconsistent with them for the 6-leg cylinder. Thus, unambiguous identification of the conformal field theory that characterizes the long-distance properties of the 6-leg cylinder is still a work in progress. (See Sec. E in SM.)

The model: We employ DMRG(35) to study the ground state properties of the Hubbard model on the square lattice, which is defined by the Hamiltonian

$$H = - \sum_{\langle ij \rangle \sigma} t_{ij} (\hat{c}_{i\sigma}^\dagger \hat{c}_{j\sigma} + h.c.) + U \sum_i \hat{n}_{i\uparrow} \hat{n}_{i\downarrow}. \quad [1]$$

Here $\hat{c}_{i\sigma}^\dagger$ ($\hat{c}_{i\sigma}$) is the electron creation (annihilation) operator on site $i = (x_i, y_i)$ with spin polarization σ , and $\hat{n}_{i\sigma}$ is the electron number operator. We take the lattice geometry to be cylindrical with periodic (open) boundary condition in the \hat{y} (\hat{x}) direction, as shown in Fig.1. $\langle ij \rangle$ denotes nearest-neighbor (NN) sites. $t_x = t$, $t_y = t + dt$, and $t'_y = t - dt$ are the electron hopping integrals between NN sites in the \hat{x} and \hat{y} directions, respectively. Here, we focus on cylinders with width L_y and

*Note that in the model as defined, the decoupled 2-leg ladder limit reached when $dt \rightarrow t$ has $t_y/t_x = 2$, which exceeds the critical value at which the Luther-Emery phase is observed; however, since this limit could be approached in multiple ways, the intuition that the finite dt state can be thought of from the perspective of weakly coupled Luther-Emery liquids is probably still valid.

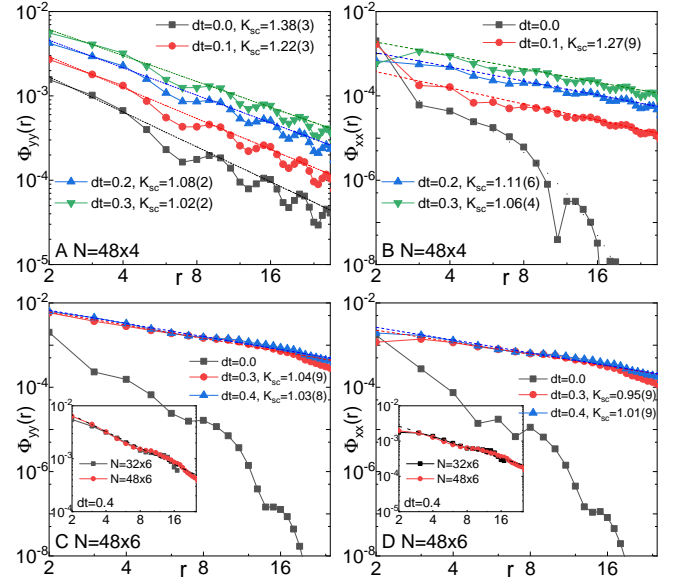


Fig. 2. Superconducting pair-field correlations. (A) $\Phi_{yy}(r; 1, 0)$ and (B) $\Phi_{xx}(r; 1, 0)$ on $N = 48 \times 4$ cylinders at $\delta = 1/12$ with different dt , (C) $\Phi_{yy}(r; 1, 0)$ and (D) $\Phi_{xx}(r; 1, 0)$ on $N = 48 \times 6$ cylinders at $\delta = 1/12$ with different dt on double-logarithmic scales. Insets: $\Phi_{yy}(r; 1, 0)$ and $\Phi_{xx}(r; 1, 0)$ in double-logarithmic scales with $dt = 0.4$ on both $N = 32 \times 6$ and $N = 48 \times 6$ cylinders. r is the distance between two Cooper pairs in the \hat{x} direction. Note that only the central-half region with $2 \leq r \leq L_x/2 + 1$ is shown and used in the fitting, whereas the remaining data points from each end are removed to minimize boundary effects. The dashed lines denote power-law fitting to $\Phi(r) \sim r^{-K_{sc}}$.

length L_x , where L_x and L_y are the number of sites along the \hat{x} and \hat{y} directions, respectively. The total number of sites is $N = L_x \times L_y$, the number of electrons is N_e , and the doping level of the system is defined as $\delta = N_h/N$, where $N_h = N - N_e$ is the number of doped holes relative to the half-filled insulator that arises when $N_e = N$.

In the present study, we chose units of energy such that $t = 1$ and consider $dt \leq 0.4$. We consider $U = 12$ at $\delta = 1/12$ and $\delta = 1/8$ doping levels and focus on $L_y = 4$ and 6 leg cylinders of length up to $L_x = 48$. We perform around 60 sweeps and keep up to $m = 20000$ states for $L_y = 4$ cylinders with a typical truncation error $\epsilon \sim 5 \times 10^{-7}$, and up to $m = 35000$ states for $L_y = 6$ cylinders with a typical truncation error $\epsilon \sim 3 \times 10^{-6}$.

The results of our calculations (as explained below) are summarized for $\delta = 1/12$ in the remaining figures and quantified in Table 1. More details, including further analysis of truncation error and results for $\delta = 1/8$, are provided in the Supplemental Material (SM).

Superconducting pair-field correlations: We have calculated the equal-time spin-singlet SC pair-field correlation function

$$\Phi_{\alpha\beta}(r; y_0, y) = \langle \Delta_\alpha^\dagger(x_0, y_0) \Delta_\beta(x_0 + r, y_0 + y) \rangle. \quad [2]$$

Here $\Delta_\alpha^\dagger(x, y) = \frac{1}{\sqrt{2}} [\hat{c}_{(x,y),\uparrow}^\dagger \hat{c}_{(x,y)+\alpha,\downarrow}^\dagger + \hat{c}_{(x,y)+\alpha,\uparrow}^\dagger \hat{c}_{(x,y),\downarrow}^\dagger]$ is the spin-singlet pair creation operator on the nearest-neighbor bond from site (x, y) oriented in the $\alpha = \hat{x}$ or \hat{y} direction. We are interested in the decay of this quantity at large distances along the cylinder, r , as a function of both the relative orientation of the two bonds, α and β , and their relative displacement transverse to the cylinder, y . We take (x_0, y_0) to be

L_y	dt	K_{sc}	Δ_d	Δ_s	Δ_π	K_{cdw}	ξ_s	ξ_G
4	0.0	1.38(3)	0.0	0.0	0.066	1.27(1)	8.6(4)	3.9(2)
4	0.1	1.22(3)	0.019	-0.011	0.074	1.35(1)	7.1(2)	3.6(2)
4	0.2	1.08(2)	0.032	-0.016	0.082	1.46(1)	4.7(2)	3.0(1)
4	0.3	1.02(2)	0.042	-0.021	0.091	1.48(1)	2.9(1)	2.5(1)
6	0.0	∞	0.0	0.0	0.0	0.3(3)	3.9(4)	2.4(3)
6	0.3	1.04(9)	0.070	0.004	0.038	3.5(2)	1.7(1)	1.8(1)
6	0.4	1.03(8)	0.062	-0.011	0.065	3.3(2)	1.3(1)	2.2(1)

Table 1. Summary of extracted parameters. The parameters are obtained by fitting the DMRG results to theoretically expected asymptotic forms of various correlation functions for $\delta = 1/12$ and the given values of L_y and dt . Exponentially falling correlations are represented by a Luttinger exponent of ∞ . Precise levels of uncertainty due to finite size effects – especially with regard to the Luttinger exponents – are difficult to estimate.

127 the “origin,” chosen to be a site near the center of the system
128 with $x_0 \sim L_x/4$ and $y_0 = 1$. At long distances ($r \gg 1$), $\Phi_{\alpha\beta}$
129 exhibits power-law decay – i.e quasi long-range order (QLRO)
130 – characterized by the Luttinger exponent K_{sc} :

$$131 \quad \Phi_{\alpha\beta}(r; y_0, y) \sim r^{-K_{sc}} \Delta_\alpha(y_0) \Delta_\beta(y_0 + y) \quad [3]$$

The nature of the pairing is encoded in the behavior of the amplitudes, $\Delta_\alpha(y)$. Specifically, were there true long-range order, i.e. in the limit $L_y \rightarrow \infty$, we could classify superconducting states, e.g. d-wave vs s-wave, by the behavior under symmetry transformations of these amplitudes. Thus, to develop some intuition concerning the meaning of these amplitudes, we analyze what they would mean in this limit. The spatial symmetries of the striped model are such that there are two inequivalent y-directed bonds and a unique x directed bond. In a state with superconducting long-range order, and if we assume that the translation symmetry of the model is not spontaneously broken, then the most general singlet order parameter on nearest-neighbor bonds can be parameterized as

$$132 \quad \begin{aligned} \Delta_y(y) &= \Delta_s + \Delta_d + e^{i\pi(y-1)} \Delta_\pi \\ \Delta_x(y) &= \Delta_s - \Delta_d \end{aligned} \quad [4]$$

133 In the limit $dt = 0$, each of these parameters would be associated with a state with different symmetries - non-zero values of Δ_s or Δ_d would characterize an “extended s-wave” or “d-wave state,” while Δ_π non-zero would correspond to a period 2 pair-density-wave aka a “ π -pairing” state. Note that, by symmetry, the pair-field vanishes on all x-directed bonds in the π -pairing state. However, for non-zero dt , the symmetry distinction between these states is removed, so some mixture of all three is expected. However, it is still reasonable (and conventional) to refer to the case in which $|\Delta_d|$ is the largest component as “d-wave-like” pairing.

134 For non-infinite L_y , the amplitudes in Eq.(3) can be viewed as reflecting the local symmetry of the pairing and as indicators of the preferred form of pairing that should be expected in the $L_y \rightarrow \infty$ limit. Importantly, for $dt = 0$, even for non-infinite L_y , there is a sharp distinction between π pairing (with $\Delta_\pi \neq 0$ and $\Delta_d = \Delta_s = 0$) and d-wave like pairing (with $\Delta_\pi = 0$ and $\Delta_d \neq 0$). To date, there is no evidence of a tendency toward π -pairing on anything other than the 4-leg cylinder. However, since for $L_y = 4$, π pairing is equivalent to d-wave pairing on plaquettes oriented perpendicular to

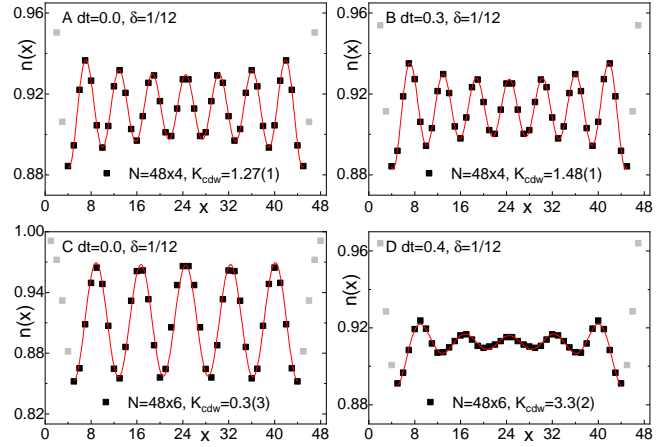


Fig. 3. Charge density profiles. Charge density distribution $n(x)$ at $\delta = 1/12$ doping level on $N = 48 \times 4$ cylinders with (A) $dt = 0.0$ and (B) $dt = 0.3$, and on $N = 48 \times 6$ cylinders with (C) $dt = 0.0$ and (D) $dt = 0.4$. The exponent K_{cdw} is extracted using Eq.(5) where the red lines are fitting curves. A few data points in light grey are neglected to minimize boundary effects.

the long axis of the cylinder, such a state has been seen and has been referred to in this context as “true d-wave”(9) or “plaquette d-wave”(13) pairing. More generally, for $dt \neq 0$, we can loosely identify distinct states by which component is largest (dominant). (These symmetry arguments are made more precise in Sec. D in SM.)

Fig.2A shows $\Phi_{yy}(r; 1, 0)$, i.e. between t_y bonds, for $L_y = 4$ cylinders at $\delta = 1/12$. The exponent K_{sc} , obtained by fitting the results using Eq.(3), is $K_{sc} = 1.38(3)$ for the uniform case, $dt = 0.0$, while for $dt = 0.2 - 0.3$, $K_{sc} \sim 1$. We have also computed other components of $\Phi_{\alpha\beta}$: $\Phi_{xx}(r; 1, 0)$ is shown in Fig.2B and $\Phi_{xy}(r; 1, 0)$ and $\Phi_{yy}(r; 1, 1)$ are shown in Fig.S2 in the SM. For the isotropic case with $dt = 0.0$, $\Phi_{xx}(r; 1, 0)$ and $\Phi_{xy}(r; 1, 0)$ decay exponentially as $\Phi_{xx}(r; 1, 0) \sim e^{-r/\xi_{sc}}$ with $\xi_{sc} \sim 1.8$,(8, 13) and $\Phi_{yy}(r; 1, y) \sim (-1)^y$, i.e. the amplitudes are consistent with π -pairing QLRO with $\Delta_\pi = 0.066$ and $\Delta_d = \Delta_s = 0$. This is consistent with previous studies of the $L_y = 4$ Hubbard and t - J models with $dt = 0$.(8, 10, 11, 13) The key new observation is that $\Phi_{xx}(r; y_0, 0)$ and $\Phi_{xy}(r; y_0, 0)$ are significantly enhanced for $dt > 0$, so that they decay as a power-law with a similar K_{sc} as Φ_{yy} . In particular, not only is K_{sc} decreased from its $dt = 0$ value, $|\Delta_d|$ increases rapidly as well. For example, for $dt = 0.3$, $\Delta_d = 0.042$, $\Delta_s = -0.021$ and $\Delta_\pi = 0.091$. (More complete results are presented in Table 1.)

The results are still more dramatic for $L_y = 6$: Consistent with previous studies on the isotropic Hubbard model, on $L_y = 6$ cylinders with $dt = 0$ we find the SC correlations are relatively weak and appear to decay exponentially with distance as shown, for $\delta = 1/12$, in Fig.2 C and D. However, as was the case for $L_y = 4$ cylinders, we find that the SC pair-field correlations are dramatically enhanced by a finite $dt > 0$, where we find that $\Phi_{\alpha\beta}(r) \sim r^{-K_{sc}}$ with $K_{sc} \sim 1$. Moreover, the SC pairing symmetry is d-wave like with $\Phi_{xx}(r) \sim \Phi_{yy}(r) \sim -\Phi_{xy}(r)$. For example, for $dt = 0.3$, $\Delta_d = 0.042$, $\Delta_s = 0.004$ and $\Delta_\pi = 0.038$. As summarized in the SM, the results we have obtained for $\delta = 1/8$ are qualitatively similar to those with $\delta = 1/12$. For instance, for $dt = 0.3$ at $\delta = 1/8$, $K_{sc} = 1.07(7)$, $\Delta_d = 0.074$, $\Delta_s = 0.007$ and $\Delta_\pi = 0.032$.

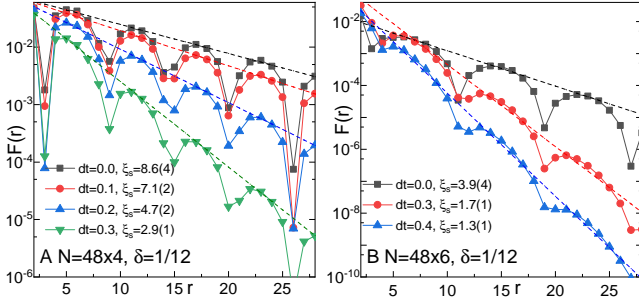


Fig. 4. Spin-spin correlations at $\delta = 1/12$. (A) $F(r)$ on $N = 48 \times 4$ cylinders with different dt , and (B) $F(r)$ on $N = 48 \times 6$ cylinders with different dt , in semi-logarithmic scale. Dashed lines denote exponential fit $F(r) \sim e^{-r/\xi_s}$, where r is the distance between two sites in the \hat{x} direction.

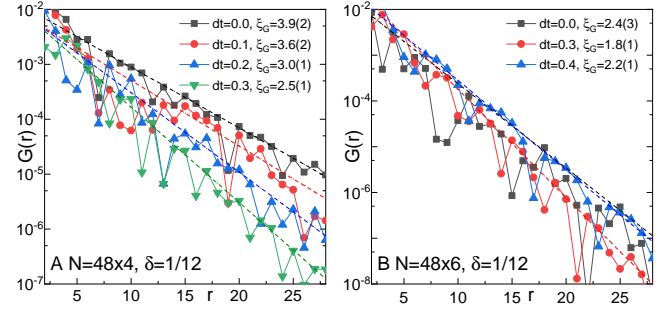


Fig. 5. Single-particle Green function at $\delta = 1/12$. (A) $G(r)$ on $N = 48 \times 4$ cylinders with different dt , and (B) $G(r)$ on $N = 48 \times 6$ cylinders with different dt on the semi-logarithmic scale. Dashed lines denote exponential fitting $G(r) \sim e^{-r/\xi_G}$ where r is the distance between two sites in the \hat{x} direction.

CDW correlations: To measure the charge order, we define the rung density operator $\hat{n}(x) = L_y^{-1} \sum_{y=1}^{L_y} \hat{n}(x, y)$ and its expectation value $n(x) = \langle \hat{n}(x) \rangle$. Fig.3A-B shows the charge density distribution $n(x)$ for $L_y = 4$ cylinders, which is consistent with “half-filled charge stripes” with wavelength $\lambda_{cdw} = 1/2\delta$. This corresponds to an ordering wavevector $Q = 4\pi\delta$, i.e. viewing the cylinder as a 1D system, 2 holes per 1D unit cell. The charge density profile $n(x)$ for $L_y = 6$ cylinders is shown in Fig.3C-D, which has wavelength $\lambda_{cdw} = 2/3\delta$, consistent with “two-third-filled” charge stripes. This corresponds to an ordering wavevector $Q = 3\pi\delta$, i.e. 4 holes per 1D unit cell.

At long distance, the spatial decay of the CDW correlation is dominated by a power-law with the Luttinger exponent K_{cdw} . The exponent K_{cdw} can be obtained by fitting the charge density oscillations induced by the boundaries of the cylinder (17, 33)

$$\begin{aligned} n(x) &= n_0 + A(x) * \cos(Qx + \phi) \\ A(x) &= A_Q * (x^{-K_{cdw}/2} + (L_x + 1 - x)^{-K_{cdw}/2}). \end{aligned} \quad [5]$$

Here A_Q is an amplitude, ϕ is a phase shift, $n_0 = 1 - \delta$ is the mean density, and $Q = 4\pi\delta$ for $L_y = 4$ cylinders and $Q = 3\pi\delta$ for $L_y = 6$ cylinders. Note that to improve the fitting quality, a few data points (corresponding to the light grey points Fig.3) are excluded to minimize the boundary effect. Values of K_{cdw} are summarized in Table 1. The fact that $K_{cdw} > K_{sc}$ for all cases in which $dt > 0$ suggests that CDW order is secondary compared with SC. The one exception is $L_y = 6$ and $dt = 0$, where the CDW correlations are at best slowly decaying and are clearly stronger than the SC. Our results are consistent with CDW QLRO with a value of $K_{cdw} \leq 0.3$, consistent with previous results for the t - J model. (14) Note that similar values of K_{cdw} can also be obtained from the asymptotic fall-off of the density-density correlation function, as shown in the SM.

Spin-spin correlations: To describe the magnetic properties of the ground state, we calculate the spin-spin correlation functions defined as

$$F(r) = \langle \vec{S}_{x_0, y_0} \cdot \vec{S}_{x_0+r, y_0} \rangle. \quad [6]$$

Here $\vec{S}_{x, y}$ is the spin operator on site $i = (x, y)$ and $i_0 = (x_0, y_0)$ is the reference site with $x_0 \sim L_x/4$. Fig.4 shows $F(r)$ for both $L_y = 4$ and $L_y = 6$ cylinders at $\delta = 1/12$ with different dt . It is clear that $F(r)$ decays exponentially

as $F(r) \sim e^{-r/\xi_s}$ at long-distances, with a finite correlation length ξ_s , i.e. there must be a finite gap in the spin sector. Moreover, ξ_s decreases with increasing dt on both $L_y = 4$ and $L_y = 6$ cylinders. In addition, we also observe for both $L_y = 4$ and $L_y = 6$ cylinders that the spin-spin correlation has spatial modulation with a wavelength λ_s that is twice that of the charge, i.e., $\lambda_s = 2\lambda_{cdw}$. Values of ξ_s for $\delta = 1/12$ and various values of dt are given in Table 1.

Single particle Green function: We have also calculated the single-particle Green function, defined as

$$G(r) = \langle c_{(x_0, y), \sigma}^\dagger c_{(x_0+r, y), \sigma} \rangle. \quad [7]$$

Fig.5 shows $G(r)$ for both $L_y = 4$ and $L_y = 6$ cylinders at $\delta = 1/12$ with different dt . The long distance behavior of $G(r)$ is consistent with exponential decay $G(r) \sim e^{-r/\xi_G}$. The extracted correlation lengths $\xi_G < 4$ for both $L_y = 4$ and $L_y = 6$ cylinders are comparable to ξ_s , as also shown in Table 1.

Summary of Results: What we have generically found, both for $L_y = 4$ and $L_y = 6$, over the entire investigated range of stripe modulation strength, dt , and doped hole concentration, δ , is a form of SC QLRO with exponentially falling spin and single particle correlations and with typically weaker, but presumably also power-law correlated CDW QLRO. Expressed in terms of the various quantities extracted by the above discussed fits of the DMRG results to theoretically expected asymptotic forms are summarized (without error bars) in Table 1.

Conclusions: It is both conceptually and practically important to understand what aspects of electronic structure are optimal for superconductivity. Circumstantial evidence has been adduced in several ways that certain organized forms of spatially inhomogeneous structure can enhance superconductivity, but we feel that the present results constitute the clearest and most unambiguous evidence to date that this is a real and robust effect. More generally, concerning the question of whether the 2d Hubbard model can support high temperature superconductivity - the present results offer encouraging evidence of an affirmative answer, as they constitute some of the strongest long-range superconducting correlations documented to date on systems wider than 4 legs. It is worth acknowledging that the present results on period 2 CDW order cannot be directly compared with the situation in the cuprates, where the CDW order typically has period closer to 3 (YBCO)

276 or 4 (BSCCO and LSCO). None-the-less, it suggests that a
277 more nuanced approach to the intertwining of CDW and SC
278 orders may be appropriate in the cuprate context.

279 Finally, there is the question of obtaining a conceptual
280 understanding of the numerical results we have reported. This
281 is an ongoing endeavor. However, it is worth mentioning a
282 possible connection between the present results, and recent
283 DMRG results that exhibit enhanced superconductivity in a
284 lightly doped quantum spin liquid.(36) Indeed, in the discus-
285 sion of the “spin-gap proximity effect” in Ref. (22), an analogy
286 was made between the effects of stripe order and a mechanism
287 based on a doped spin liquid.

288 It is reasonable to conclude that the low energy magnetic
289 fluctuations associated with antiferromagnetic order or near
290 order (i.e. with energies small compared to the SC gap), are
291 detrimental to SC - they would generally be expected to be pair-
292 breaking.(37) However, higher energy, short-range correlated
293 antiferromagnetic fluctuations can produce precisely the sort
294 of momentum dependent interactions that are most conducive
295 to d-wave SC. In this sense, a fully gapped spin liquid would
296 seem to have just the right spectrum of magnetic fluctuations
297 to be an optimal parent to a high temperature superconductor.
298 Indeed, it is possible to view the gap in such a state as the
299 pairing gap of a superconductor that is waiting to be liberated.
300 In a similar sense, the undoped ($\delta = 0$) two-leg Hubbard
301 ladder has a spin-gap and can be viewed as a Mott insulator of
302 preexisting Cooper pairs (rung singlets). In this sense, doping
303 into a modulated array of effective two leg ladders may be
304 analogous to doping a fully gapped quantum spin liquid.

305 **ACKNOWLEDGMENTS.** We would like to thank Dror Orgad,
306 Vladimir Calvera, Richard Scalettar, Doug Scalapino, John Tran-
307 quada and Thomas Devereaux for helpful discussions. This work
308 was supported by the Department of Energy, Office of Science, Bas-
309 ic Energy Sciences, Materials Sciences and Engineering Division,
310 under Contract DE-AC02-76SF00515.

311 1. E. Fradkin, S. A. Kivelson, and J. M. Tranquada. Colloquium: Theory of intertwined orders in
312 high temperature superconductors. *Rev. Mod. Phys.* **87**, 457–482 (2015).
313 2. D. P. Arovas, E. Berg, S. A. Kivelson, and S. Raghu. The Hubbard Model. *arXiv:2103.12097*
314 (2021).
315 3. M. Qin, T. Schäfer, S. Andergassen, P. Corboz, and E. Gull. The Hubbard model: A compu-
316 tational perspective. *arXiv:2104.00064* (2021).
317 4. B. Keimer, S. A. Kivelson, M. R. Norman, S. Uchida, and J. Zaanen. High Temperature
318 Superconductivity in the Cuprates. *Nature* **518**, 179 (2015).
319 5. S. R. White and D.J. Scalapino. Competition between stripes and pairing in a t - t' - J model.
320 *Phys. Rev. B* **60**, R753–R756 (1999).
321 6. D. J. Scalapino and S. R. White. Stripe structures in the t - t' - J model. *Physica C: Supercon-*
322 *ductivity*, **481**, 146 – 152 (2012).
323 7. G. Hager, G. Wellein, E. Jeckelmann, and H. Fehske. Stripe formation in doped Hubbard
324 ladders. *Phys. Rev. B* **71**, 075108 (2005).
325 8. H. C. Jiang, Z. Y. Weng, and S. A. Kivelson. Superconductivity in the doped t - J model:
326 Results for four-leg cylinders. *Phys. Rev. B* **98**, 140505 (2018).
327 9. J. F. Dodaro, H. C. Jiang, and S. A. Kivelson. Intertwined order in a frustrated four-leg t - J
328 cylinder. *Phys. Rev. B* **95**, 155116 (2017).
329 10. H. C. Jiang and T. P. Devereaux. Superconductivity in the doped Hubbard model and its
330 interplay with next-nearest hopping t' . *Science* **365**, 1424–1428 (2019).
331 11. Y. F. Jiang, J. Zaanen, T. P. Devereaux, and H. C. Jiang. Ground state phase diagram of the
332 doped hubbard model on the four-leg cylinder. *Phys. Rev. Research* **2**, 033073 (2020).
333 12. B. X. Zheng, C. M. Chung, P. Corboz, G. Ehlers, M. P. Qin, R. M. Noack, H. Shi, S. R. White,
334 S. Zhang, and G. K. L. Chan. Stripe order in the underdoped region of the two-dimensional
335 Hubbard model. *Science* **358**, 1155–1160 (2017).
336 13. C. M. Chung, M. Qin, S. Zhang, U. Schollwöck, and S. R. White. Plaquette versus ordinary
337 d -wave pairing in the t' -Hubbard model on a width-4 cylinder. *Phys. Rev. B* **102**, 041106
338 (2020).
339 14. M. Qin, C. M. Chung, H. Shi, E. Vitali, C. Hubig, U. Schollwöck, S. R. White, and S. Zhang.
340 Absence of superconductivity in the pure two-dimensional Hubbard model. *Phys. Rev. X* **10**,
341 031016 (2020).
342 15. S. Jiang, D. J. Scalapino, and S. R. White. Ground State Phase Diagram of the t - t' - J model.
343 *arXiv:2104.10149* (2021).
344 16. H. C. Jiang, S. Chen, and Z. Yu Weng. Critical role of the sign structure in the doped mott in-
345 sulator: Luther-emery versus Fermi-liquid-like state in quasi-one-dimensional ladders. *Phys.*
346 *Rev. B* **102**, 104512 (2020).

17. S. S. Gong, W. Zhu, and D. N. Sheng. Robust d -wave superconductivity in the square-lattice
347 t - J model. *Phys. Rev. Lett.* **127**, 097003 (2021). 348
18. A. Luther and V. J. Emery. Backward scattering in the one-dimensional electron gas. *Phys.*
349 *Rev. Lett.* **33**, 589–592 (1974). 350
19. E. Fradkin and S. A. Kivelson. High-temperature superconductivity: Ineluctable complexity.
351 *Nat. Phys.* **8**, 864–866 (2012). 352
20. C. Catellani, C. DiCastro, and M. Grilli. Singular quasi-particle scattering in the proximity of
353 charge instabilities. *Phys. Rev. Lett.* **75**, 4650–4653 (1995). 354
21. A. Perali, C. Castellani, C. DiCastro, and M. Grilli. d -wave superconductivity near charge
355 instabilities. *Phys. Rev. B* **54**, 16216–16225 (1996). 356
22. V. J. Emery, S. A. Kivelson, and O. Zachar. Spin-gap proximity effect mechanism of high-
357 temperature superconductivity. *Phys. Rev. B* **56**, 6120–6147 (1997). 358
23. E. Arrigoni, E. Fradkin, and S. A. Kivelson. Mechanism of high-temperature superconductivity
359 in a striped Hubbard model. *Phys. Rev. B* **69**, 214519 (2004). 360
24. S. A. Kivelson and E. Fradkin. How optimal inhomogeneity produces high temperature super-
361 conductivity. *arXiv:cond-mat/0507459* (2005). 362
25. T. Ying, R. Mondaini, X. D. Sun, T. Paiva, R. M. Fye, and R. T. Scalettar. Determinant quantum
363 Monte Carlo study of d -wave pairing in the plaquette Hubbard Hamiltonian. *Phys. Rev. B* **90**,
364 075121 (2014). 365
26. S. Baruch and D. Orgad. Contractor-renormalization study of Hubbard plaquette clusters.
366 *Phys. Rev. B* **82**, 134537 (2010). 367
27. G. Wachtel, S. Baruch, and D. Orgad. Optimal inhomogeneity for pairing in Hubbard systems
368 with next-nearest-neighbor hopping. *Phys. Rev. B* **96**, 064527 (2017). 369
28. W. F. Tsai, H. Yao, A. Laeuchli, and S. A. Kivelson. Optimal inhomogeneity for superconduc-
370 tivity: Finite-size studies. *Phys. Rev. B* **77**, 214502 (2008). 371
29. J. Zaanen, and O. Gunnarsson. Charged magnetic domain lines and the magnetism of high-
372 T_c oxides. *Phys. Rev. B* **40**, 7391–7394 (1989). 373
30. Kazushige Machida. Magnetism in La_2CuO_4 based compounds. *Physica C: Superconductivity*
374 **158**, 192–196 (1989). 375
31. Masaru Kato, Kazushige Machida, Hiizu Nakanishi, and Mitsutaka Fujita. Soliton lattice mod-
376 ulation of incommensurate spin density wave in two dimensional hubbard model -a mean field
377 study-. *Journal of the Physical Society of Japan*, **59**, 1047–1058 (1990). 378
32. R. M. Noack, S. R. White, and D. J. Scalapino. The doped two-chain Hubbard model. *EPL*
379 (*Europhysics Letters*) **30**, 163–168 (1995). 380
33. S. R. White, I. Affleck, and D. J. Scalapino. Friedel oscillations and charge density waves in
381 chains and ladders. *Phys. Rev. B* **65**, 165122 (2002). 382
34. M. Dolfi, B. Bauer, S. Keller, and M. Troyer. Pair correlations in doped Hubbard ladders. *Phys.*
383 *Rev. B* **92**, 195139 (2015). 384
35. S. R. White. Density matrix formulation for quantum renormalization groups. *Phys. Rev. Lett.*
385 **69**, 2863–2866 (1992). 386
36. H. C. Jiang and S. A. Kivelson. High Temperature Superconductivity in a Lightly Doped
387 Quantum Spin Liquid. *Phys. Rev. Lett.* **127**, 097002 (2021). 388
37. For a clear discussion see P. Monthoux and D.J.Scalapino, Variations of T_c for changes in
389 the spin-fluctuation spectral weight. *Phys. Rev. B* **50**, 10339 (1994). 390